Available online at www.sciencedirect.com
SCIENCE DIRECT®
International Journal of Heat and Fluid Flow 24 (2003) 91–99
International Journal of HEAT AND FLUID FLOW
www.elsevier.com/locate/ijhff

Film cooling from two rows of holes with opposite orientation angles: injectant behavior and adiabatic film cooling effectiveness

Joon Ahn, In Sung Jung, Joon Sik Lee *

School of Mechanical and Aerospace Engineering, Seoul National University Seoul 151-742, South Korea

Received 5 July 2001; accepted 14 June 2002

Abstract

The present paper is aiming at describing the injectant behaviors from two rows of film cooling holes with opposite orientation angles. Boundary layer temperature distributions were measured in the streamwise normal plane to illustrate the interaction between the injectant from the holes in the upstream row and from the downstream row. Detailed adiabatic film cooling effectiveness distributions were also measured using thermochromic liquid crystal to investigate how well the injectant covers the film cooled surface. Four film cooling hole arrangements were considered including inline and staggered ones. And three blowing ratios of 0.5, 1.0 and 2.0 were studied. At the blowing ratio of 0.5, the injectant is centered near film cooled surface irrespective of hole configurations to show high film cooling effectiveness. When the blowing ratio exceeds unity the injectant tends to lift off from the wall due to the increase of the wall normal momentum. With the inline configuration, not like other configurations, the injectant is still well attached to the wall with the help of the downwash flow formed at the hole exit.

Keywords: Film cooling; Compound angle injection; Injectant behavior; Adiabatic film cooling effectiveness

1. Introduction

The efficiency of gas turbine depends highly on the turbine inlet temperature, but the inlet temperature is limited to the allowable temperature of blade material. Film cooling is commonly used to prevent thermal failure in turbine blades that could result from the operation in high temperature environment. In film cooling, the cooling air bled from the compressor is discharged through holes in the turbine blade wall or the end wall. The injected coolant from holes form a thin thermal insulation layer on the blade surface to protect the blade from being overheated by the hot gas flow from the combustor. The film cooling effectiveness is known to be affected by blade geometry, injection hole configuration, approaching flow characteristics, coolant to approaching flow velocity ratio, to name a few.

The compound angle injection can be identified by two angles as illustrated in Fig. 1. The inclination angle (α) is defined as the angle between the injection vector and its projection on x–z plane whereas the orientation angle (β) is defined as the angle between the streamwise direction and the projection of the injection vector on x–z plane. In the compound angle orientation system, the coolant is injected with a spanwise momentum component. The compound angle holes, thus, provide more uniform film coverage in the spanwise direction. As the orientation angle increases the counter-rotating vortices, which usually observed in the simple angle injection system ($\beta = 0$), merge into a single strong vortex and the strength of downstream secondary flow depends strongly on the velocity ratio (Lee et al., 1997). The previous studies, in general, show that compound angle injection provides substantially improved effectiveness compared with simple angle injection for the same spanwise hole spacing, normalized streamwise location and blowing ratio (Honami et al., 1994; Schmidt et al., 1996; Ekkad et al., 1997b). It is also noteworthy that the film coolant injected from compound angle holes interacts with the mainstream fluid more vigorously to increase the heat transfer coefficient (Sen et al., 1996; Ekkad et al., 1997a).

* Corresponding author. Tel.: +82-2-880-7117; fax: +82-2-883-0179.
E-mail address: jslee@gong.snu.ac.kr (J.S. Lee).

0142-727X/02/$ - see front matter © 2002 Elsevier Science Inc. All rights reserved.
PII: S0142-727X(02)00200-X

Nomenclature

D	film hole diameter
H	shape factor
L	film cooling hole length measured along the hole centerline
M	blowing ratio
Re_D	Reynolds number based on film cooling hole diameter
T	temperature
U	velocity
x	streamwise distance from center point of film cooling hole exit
y	normal distance from the wall
z	lateral distance from centerline of the film cooling hole

Greeks

α	inclination angle
β	orientation angle
δ	boundary layer thickness, 99% point
δ^*	displacement thickness
η	adiabatic film cooling effectiveness
ν	kinematic viscosity
θ	momentum thickness
Θ	dimensionless boundary layer temperature

Subscripts

∞	freestream conditions
aw	adiabatic wall conditions

Superscripts

$-$	laterally averaged value
$=$	spatially averaged value

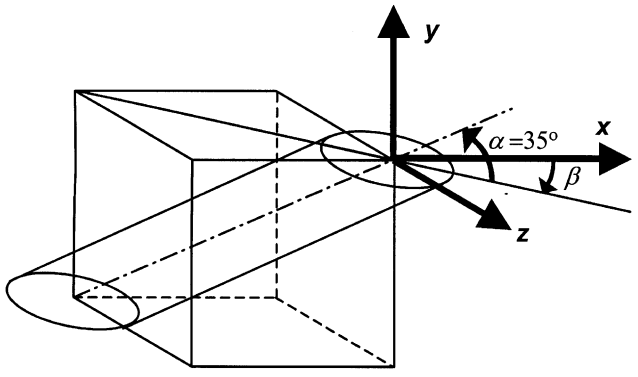

Fig. 1. Configuration of compound angle injection.

The rows of film cooling holes are arranged in groups of closely spaced holes. In common practice there are as few as one and as many as five rows in a group (Muska et al., 1976). In the absence of experimental data, the adiabatic effectiveness values of multi-row injection are usually evaluated by a superposition method using data from two or more films as suggested by Sellers (1963). The superposition method, however, cannot be applied to full three dimensional flow at the downstream of the hole exit. Flow field measurements show that the dominant structures identified in the flowfield downstream of the first row were also present behind the second row (Sinha et al., 1991). There might exist large differences in film cooling performance between staggered and inline configurations. The staggered configuration showed better performance than the inline configuration for the simple angle injection (Afejuku et al., 1983). In the film cooling from two rows of holes, the compound angle injection provides significantly improved protection compared to simple angle configuration (Ligrani et al., 1994).

The previous studies on the film cooling from two rows of holes with compound angle injection mainly adopted staggered configuration. They made each row of holes have the same orientation angles. Since the injectant from the compound angle holes possesses lateral momentum component, the injectant trajectory moves in the z-direction as it flows downstream. Thus, effects of configuration on film cooling can be different from that of simple angle injection.

In the present study, two rows of holes with oppossite orientation angles are employed to investigate the interactions of injectant flow with vortices. Four different hole configurations including inline and staggered ones are investigated. The effect of three blowing ratios is also considered for all configurations.

2. Experimental apparatus and procedures

An open type subsonic wind tunnel is used to generate the free-stream as shown in Fig. 2(a). A boundary layer trip wire of 1.8 mm diameter is located at $20D$, where D is the hole diameter, upstream from downstream holes to provide a turbulent boundary layer flow at the exit of the holes. The air, used as the injectant, first flows through an orifice followed by two heat exchangers that control the injectant temperature. Then, the air is ducted to a plenum chamber and discharged through the injection holes. Experimental conditions are summarized in Table 1.

The bottom plate of the duct consists of an upstream plate, a coolant exit plate, and a measurement plate (see Fig. 2(b)). Fig. 3 shows film hole arrangement on coolant exit plates prepared for each configuration. Configuration 1 is inline and configuration 3 is staggered one.

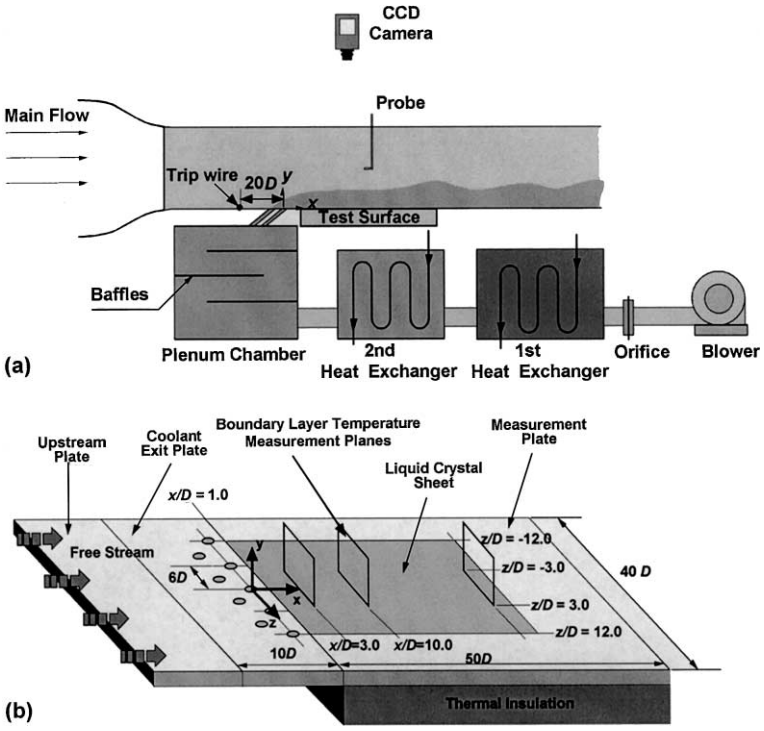

Fig. 2. Schematic diagram of experimental setup: (a) schematic diagram of wind tunnel and coolant supply system; (b) configuration of measurement plate.

Table 1
Experimental conditions

U_∞	10 m/s
D	10 mm
δ/D	1.50
$H\ (=\delta^*/\theta)$	1.36
L/D	4.0
$M\ (=\rho_c U_c/\rho_\infty U_\infty)$	0.5, 1.0, 2.0
$Re_D\ (=U_\infty D/v)$	6570
$Re_\theta\ (=U_\infty \theta/v)$	957

Configurations 2 and 4 are the arrangements between the inline and the staggered. The space between rows is set to be $4D$, commonly found in the previous studies such as Ligrani et al. (1994). The space between holes in a row is chosen as $6D$, which is relatively wide, in order to clearly see the interaction between the injectants.

The boundary layer temperature distribution can reveal information about injectant behaviors and has a close relation with film cooling effectiveness distribution on the surface. In the measurement of boundary layer temperature distribution and the adiabatic film cooling effectiveness, free-stream temperature is fixed at 20 °C while the injectant is heated to 40 °C. The boundary layer temperature distribution is described in terms of dimensionless temperature defined as follows:

$$\Theta = \frac{T - T_\infty}{T_c - T_\infty} \tag{1}$$

Boundary layer temperature distributions are measured using T-type thermocouples calibrated in a constant temperature bath with a precision platinum resistance thermometer. The boundary layer temperature distribution is measured at $x/D = 3.0$, in $-3.0 \leqslant z/D \leqslant 3.0$.

The adiabatic film cooling effectiveness is defined as follows:

$$\eta = \frac{T_{aw} - T_\infty}{T_c - T_\infty} \tag{2}$$

where T_{aw} denotes the adiabatic wall temperature. The effectiveness value of 1.0 denotes that the adiabatic wall temperature is the same as the coolant temperature which implies that the wall is perfectly protected by the coolant.

For the effectiveness measurements, the injectant is heated by 20 °C higher than the free-stream temperature. Both free-stream temperature (T_∞) and injectant temperature (T_c) are measured with T-type thermocouples. The adiabatic wall temperature is measured using thermochromic liquid crystal (TLC). The TLC sheet is covered in the range $1.0 \leqslant x/D \leqslant 31.0$, and $-12.0 \leqslant z/D \leqslant 12.0$. This measuring technique provides temperature distributions of the entire surface of interest at a time.

There are various techniques of TLC used for temperature measurements. Among them, a transient technique has been used by Ekkad et al. (1997a,b) and the steady state, hue capturing technique is adopted in the

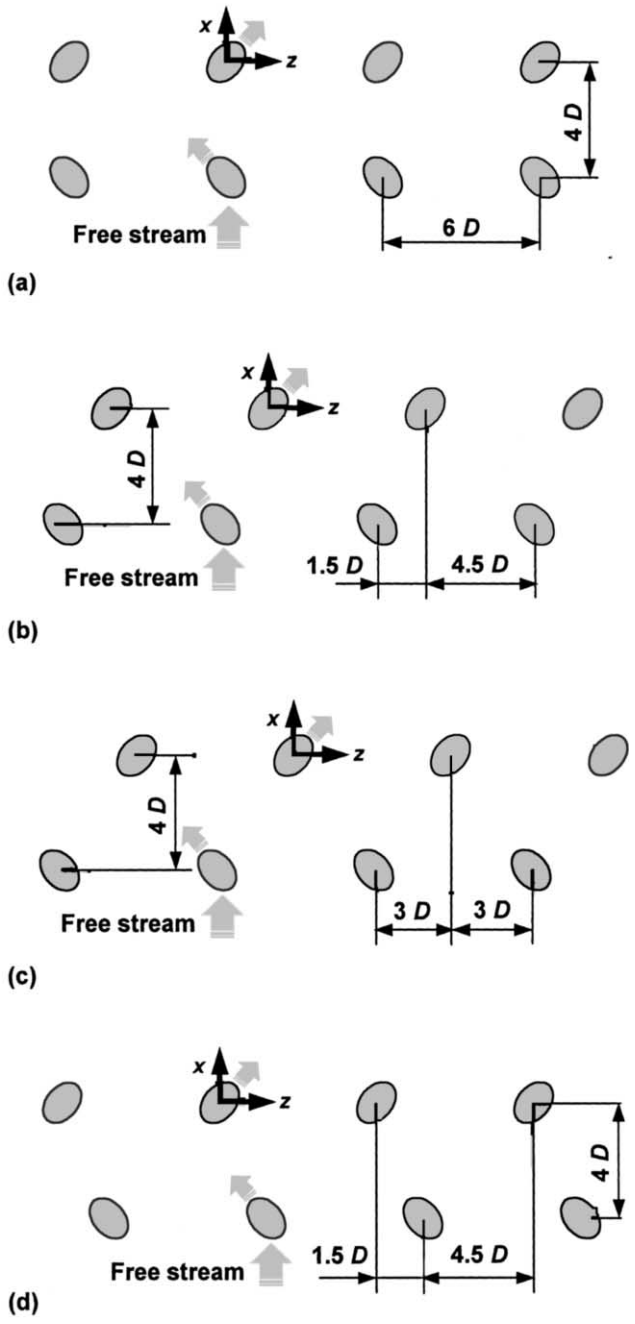

Fig. 3. Injection hole geometries: (a) configuration 1; (b) configuration 2; (c) configuration 3; (d) configuration 4.

present study. Every TLC has a color play temperature range and we used a wide band TLC sheet. With the help of wide band width we can map the entire isothermal pattern from a single image but a robust calibration is indispensable for the high accuracy measurement. Prior to the data acquisition, the wind tunnel and the injectant blower are activated to allow the surface temperature to reach a steady state. The process typically takes 2 h. The TLC color image is then captured by a CCD camera for 30 s. From the captured images, the hue values are calculated and time-averaged simultaneously. The hue values are then converted to temperature.

The uncertainty analysis is evaluated on 20 to 1 odds (95% confidence level). All the uncertainty values are evaluated based on single-sample experiments proposed by Kline and McClintock (1953). The uncertainty of the dimensionless boundary layer temperature is estimated at a typical dimensionless boundary layer temperature value of 0.25. The uncertainty of dimensionless temperature is 5.7%, and of the adiabatic film cooling effectiveness is 6.8% at a typical η value of 0.2.

3. Results and discussion

3.1. Boundary layer temperature distribution

With the two rows of holes, the flow formed at the downstream hole exit is not supposed to be a simple turbulent boundary layer flow any more. The injectant from the holes in the upstream row will establish a different flow condition at the downstream hole exit according to the blowing ratio and hole arrangement. To illustrate the flow condition at the downstream hole exit, boundary layer temperature field is measured at the downstream hole exit ($x/D = 0.0$) while heating the injectant and blocking the downstream holes. Then, the temperature field represents the injectant concentration distribution from upstream holes at the location.

Since the upstream holes have orientation angles of $-45°$ (see Fig. 4(a)), the injectant from upstream holes is supposed to have a clockwise vortex. The vortex forms a downwash flow on the right side of the jet and an upwash flow on the left, which results in the asymmetric shapes of temperature distributions shown in Fig. 4. With an increase in the blowing ratio, the vortex is strengthened and the injectant lifts off from the wall. Thus, the effect of the vortex is most conspicuous at the blowing ratio of 2.0 (see Fig. 4(c)). The secondary flow entrains the free-stream to form a low temperature region around $z/D = -1.5$ and $y/D = 0.5$.

The injectant trajectory moves in the negative z-direction as it flows downstream since the injectant from a compound angle hole has a lateral component of momentum. Accordingly, the downwash regions of the upstream injectant are located at the downstream-hole exits for configuration 1 ($z/D = 0$ in Fig. 4) at the blowing ratios of 1.0 and 2.0. For configuration 4 ($z/D = -1.5$ in Fig. 4), however, injectant from downstream holes encounters upwash flow at the hole exit. For the staggered configuration (configuration 3), the downstream hole exit is free of injectant from upstream row at the blowing ratio of 0.5. The injectant, however, is confronted by the upwash flow as the blowing ratio increases to 2.0. For configuration 2, the downwash flow

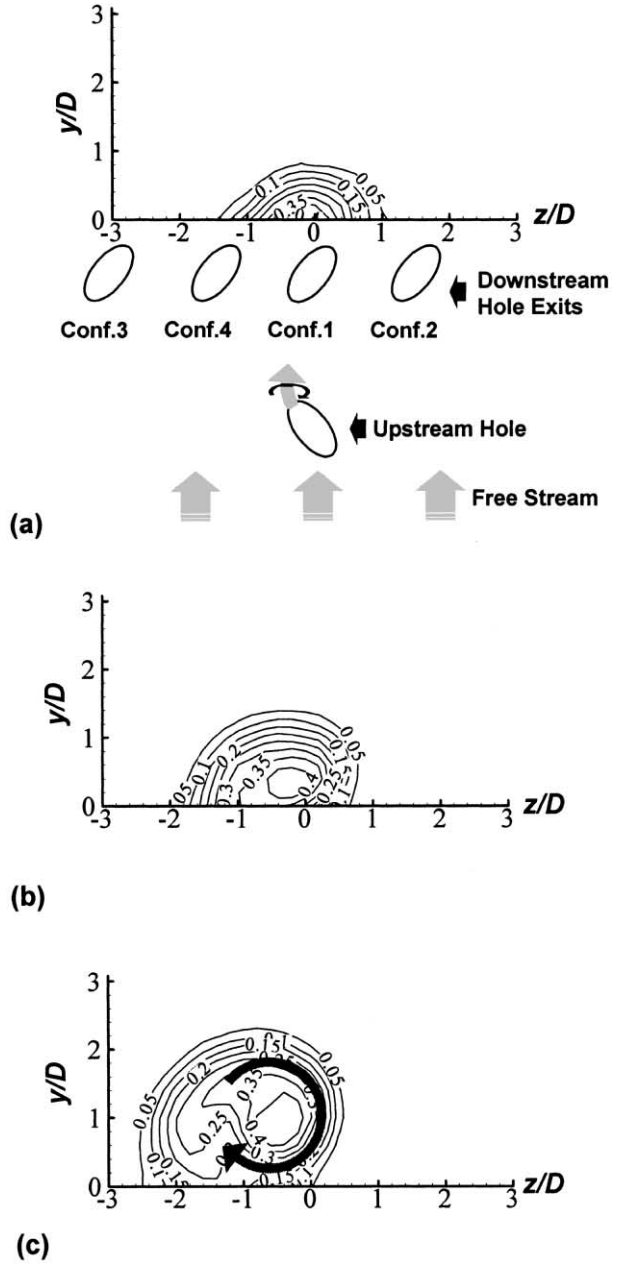

Fig. 4. Boundary layer temperature distributions at downstream hole exit: (a) $M = 0.5$; (b) $M = 1.0$; (c) $M = 2.0$.

is located at downstream hole exits at the blowing ratio of 0.5.

As depicted above, each configuration has different flow condition at the downstream hole exit according to the blowing ratio. The injectant from the downstream holes behaves differently according to the blowing ratio and configuration as shown in Fig. 5. At the blowing ratio of 0.5 (Fig. 5(a)), the injectant is attached fairly well to the wall and confined to $y/D \approx 1.5$ irrespective of configurations. The injectant lifts slightly off the wall at $M = 1.0$ comparing to at $M = 0.5$. This is simply because the injectant at $M = 1.0$ has a larger normal momentum component than at $M = 0.5$. For the inline configuration (configuration 1), however, the injectant is centered near the surface at $M = 1.0$ due to the downwash flow formed at the hole exit. As the blowing ratio increases to 2.0, injectant penetration is so apparent that $\Theta = 0.05$ contour line rises to $y/D \approx 3.0$.

Near wall values of nondimensional temperature Θ are of particular importance because they approach local magnitude of the surface adiabatic film cooling effectiveness. At the blowing ratio of 0.5, the maximum Θ level that meets the surface is about 0.5 for all configurations. Thus, the key factor that determines overall film cooling effectiveness is not the maximum wall level of Θ but the area of unprotected region. High spanwise-averaged film cooling effectiveness is expected for the configurations 2 and 3, whose unprotected areas are relatively narrow. Configuration effect is more significant at higher blowing ratios. For configuration 1, the width surrounded by $\Theta = 0.5$ contour line increased to cover the range of $-1.0 \leqslant x/D \leqslant 0.2$ at $M = 1.0$. For the other configurations, however, maximum Θ levels at $y/D = 0$ decreased as the blowing ratio increases to 1.0 because the injectant is getting detached from the wall. At the blowing ratio of 2.0, the configuration effect is most distinct. The injectant is still well attached to the wall with the inline configuration though not as well as at the blowing ratio of 1.0. For configurations 3 and 4, a wide range of unprotected region is observed. An interesting fact here is that the injectant distribution of configuration 4 at $M = 1.0$ looks similar to that of configuration 3 at $M = 2.0$. This is because the injectant with higher blowing ratio has more lateral momentum to move more in spanwise direction as it flows downstream.

3.2. Adiabatic film cooling effectiveness

The film cooling effectiveness distributions for $M = 0.5$ are shown in Fig. 6. The overall characteristics of the effectiveness distributions are the high level of effectiveness compared to other blowing ratios. The high effectiveness value results from the attachment of the injectant to the wall as shown in the boundary layer temperature distributions (see Fig. 5). The differences in the adiabatic film cooling effectiveness value with respect to the configurations are not significant because the injectant is well attached to the wall for all investigated configurations. However, the distribution, which explains the uniformity of adiabatic film cooling effectiveness, shows difference with respect to the configuration. The inline configuration and configuration 4 show a wide less-protected area surrounded by the contour of $\eta = 0.15$, whereas configuration 2 provides a more uniform effectiveness distribution.

When the velocity ratio increases to 1.0, the film cooling performance of each configuration becomes

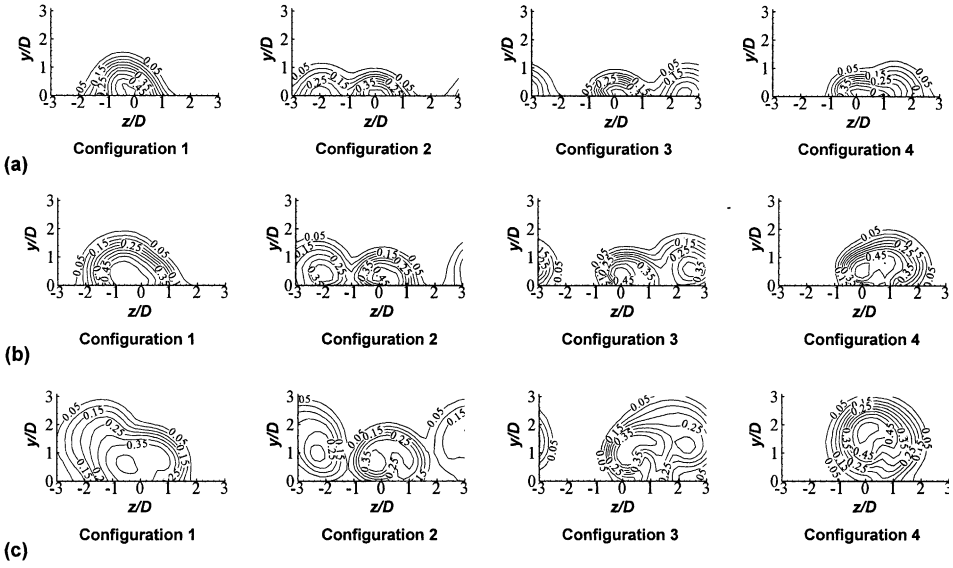

Fig. 5. Boundary layer temperature distributions with two rows of holes at $x/D = 3.0$: (a) $M = 0.5$; (b) $M = 1.0$; (c) $M = 2.0$.

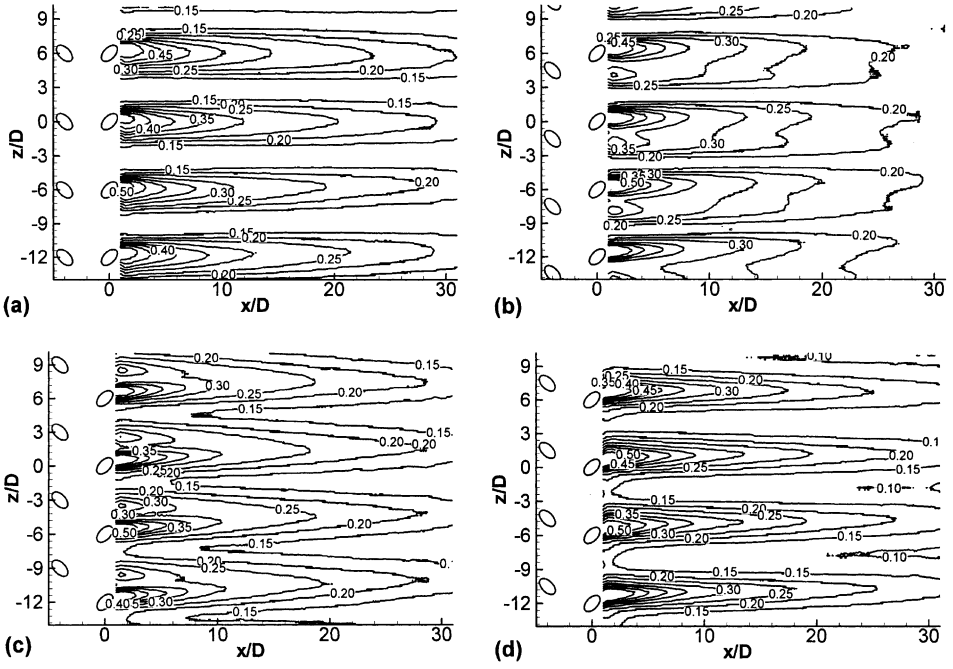

Fig. 6. Adiabatic film cooling effectiveness distributions for $M = 0.5$: (a) configuration 1; (b) configuration 2; (c) configuration 3; (d) configuration 4.

more distinct as illustrated in Fig. 7. The injectant starts to lift off from the wall for configurations 3 and 4, while it is still well attached to the wall with the inline configuration (see Fig. 5). Consequently, configuration 1 shows high film cooling effectiveness values. Between holes, however, there exist triangular areas surrounded by the contour of $\eta = 0.15$ where the surface is less protected by the injectant. Configuration 2 shows more uniform effectiveness distributions in the vicinity of the holes than the inline configuration. But the overall effectiveness level is lowered compared to that of configuration 1. The lift-off of the injectant causes a decrease in the effectiveness level more significantly with configurations 3 and 4. For both of the configurations, wide less protected areas surrounded by the contour of $\eta = 0.10$ are observed where x/D exceeds 0.5.

Fig. 8 shows the adiabatic film cooling effectiveness distributions at the blowing ratio of 2.0, which varies remarkably according to the configuration due to the stronger vortex motion. Configuration 1 shows higher effectiveness level than other configurations because of the downwash flow at the hole exit. Another interesting

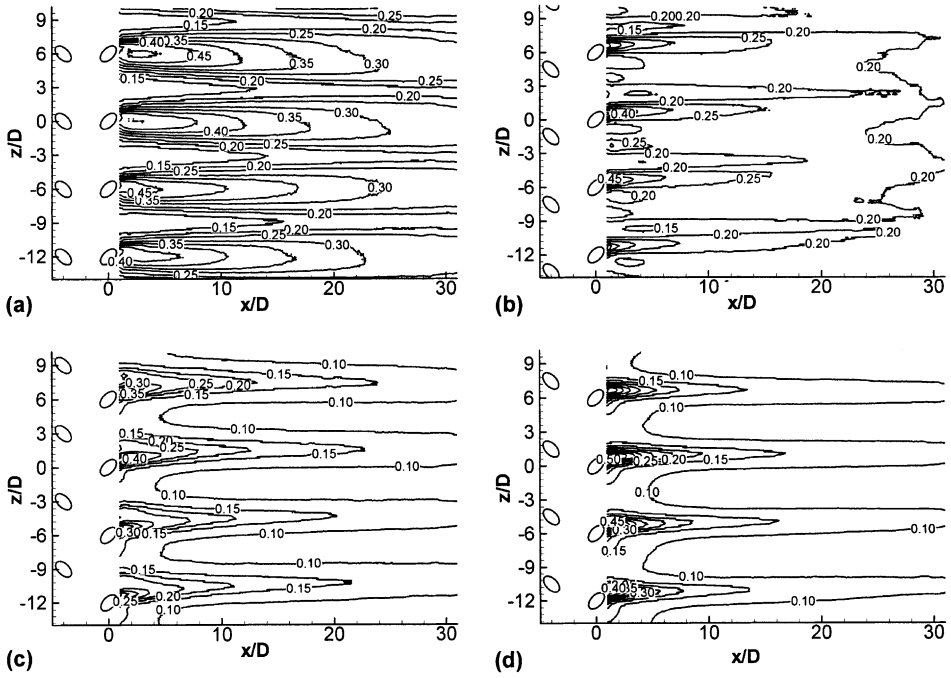

Fig. 7. Adiabatic film cooling effectiveness distributions for $M = 1.0$: (a) configuration 1; (b) configuration 2; (c) configuration 3; (d) configuration 4.

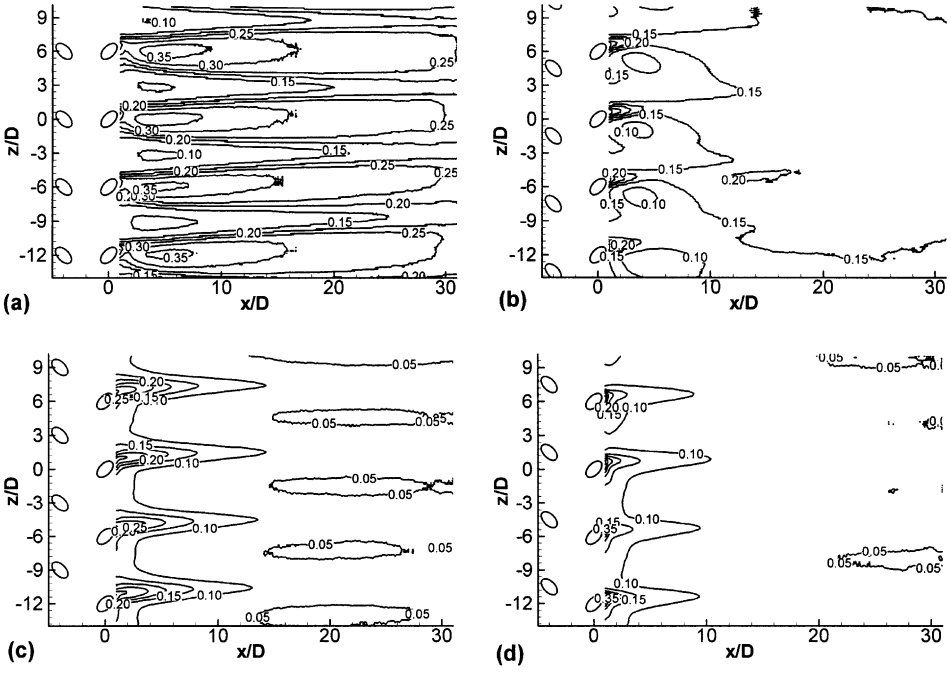

Fig. 8. Adiabatic film cooling effectiveness distributions for $M = 2.0$: (a) configuration 1; (b) configuration 2; (c) configuration 3; (d) configuration 4.

feature of the effectiveness distribution at $M = 2.0$ is the re-increase of the effectiveness. For configuration 1, $\eta = 0.35$ contours (the highest effectiveness level) are observed from $x/D \cong 3.0$ to indicate that the re-increase begins at $x/D \cong 3.0$. For configuration 2, the re-increase of effectiveness can be found at $x/D \cong 10.0$ judging from $\eta = 0.15$ contour. However, it can be hardly observed in the cases of configurations 3 and 4.

Fig. 9 compares the laterally averaged film cooling effectiveness for inline and staggered configurations with data from Ligrani et al. (1994). Ligrani et al. (1994) presented results for two staggered rows of holes with

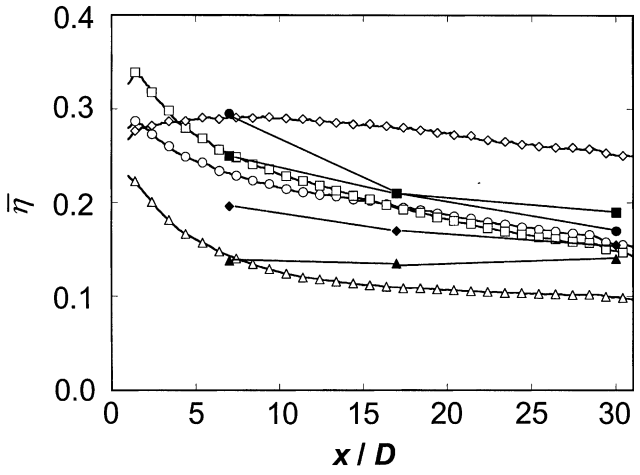

Fig. 9. Spanwise-averaged adiabatic film cooling effectiveness: ○, configuration 1 ($M = 0.5$); □, configuration 3 ($M = 0.5$); ◇, configuration 1 ($M = 1.0$); △, configuration 3 ($M = 1.0$); ●, Ligrani et al. (1994) ($M = 0.5$, $\beta = 50.5°$); ■, Ligrani et al. (1994) ($M = 1.0$, $\beta = 50.5°$); ◆, Ligrani et al. (1994) ($M = 0.5$, $\beta = 0°$); ▲, Ligrani et al. (1994) ($M = 1.0$, $\beta = 0°$).

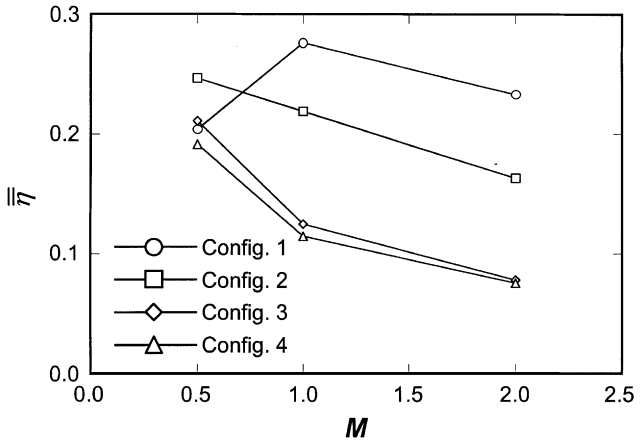

Fig. 10. Space-averaged film cooling effectiveness.

the same hole and row spacing as the present study. The major difference from the present study is that they set the orientation angle as 0° (simple angle) or 50.5° for all holes in the both of rows. At the blowing ratio of 0.5, spanwise uniformity is so important that configuration 3 (hollow rectangular symbol) shows higher film cooling effectiveness than configuration 1 (hollow circular symbol) till $x/D = 15$. When compared with the data of Ligrani et al. (1994), the present results lie between simple and compound angle results for $M = 0.5$. At the blowing ratio of 1.0, on the contrary, their results lie between the present results for configurations 1 and 3.

Goldstein et al. (1968) reported that the highest adiabatic film cooling effectiveness is obtained at the blowing ratio of 0.5 from a simple angle cylindrical hole with the inclination angle of 35°. With two rows of holes, Jabbari and Goldstein (1978) described that for $x/D > 12.5$ the centerline effectiveness increases with increasing blowing ratio and levels off when $M > 1.0$. The results from Ligrani et al. (1994) shows the adiabatic effectiveness at $M = 0.5$ is greater than at $M = 1.0$ till $x/D = 30$ for simple angle injection (see solid diamond and triangular symbol in Fig. 9). This discrepancy is considered to be caused mainly by the difference in the hole spacing. For the compound angle, the film cooling effectiveness at $M = 1.0$ exceeds one at $M = 0.5$ beyond $x/D \cong 17$. In the present study, the film cooling effectiveness at $M = 0.5$ is higher than at $M = 1.0$ for configuration 3 throughout the measured surface. However, the trend is reversed behind $x/D \cong 2.0$ for the configuration 1 (inline).

A space averaged adiabatic effectiveness was used to compare the film cooling performance of different configurations over a wide range of blowing ratios. Fig. 10 shows the space-averaged effectiveness which is determined by averaging the effectiveness in the region of $-3.0 \leqslant z/D \leqslant 3.0$ and $1.0 \leqslant x/D \leqslant 31.0$. For the inline configuration (configuration 1) the space-averaged effectiveness is higher by 40% at $M = 1.0$ than at $M = 0.5$. For other configurations, the space averaged effectiveness decreases as the blowing ratio increases from 0.5 to 2.0. Configuration 2, however, yields higher effectiveness than those of configurations 3 and 4. Since the upwash flow at the hole exit enhances the injectant lift-off at the high blowing ratio for configurations 3 and 4, the effectiveness decreases drastically as the blowing ratio increases.

4. Conclusions

The film cooling performance is evaluated for film hole configurations with opposite orientation angles, and the effect of blowing ratios on boundary layer temperature distribution are investigated. Some important observations are noticed and summarized below.

1. At the blowing ratio of 0.5, the injectant is centered near the surface regardless of the configuration to provide high adiabatic effectiveness level. Therefore, the spatial uniformity is more significant factor to determine the overall film cooling effectiveness than local film cooling effectiveness level.
2. At the higher blowing ratios of 1.0 and 2.0, the interaction between injectant from the upstream and downstream holes becomes important to film cooling effectiveness. The downwash flow at the hole exit makes the injectant well attached to the wall to yield the high film cooling effectiveness, whereas the upwash flow deteriorates it. Consequently, configuration 1 provides high adiabatic film cooling effectiveness, while configurations 3 and 4 show lower values.

3. For the film cooling with two rows of holes, the previous data usually showed that the lower blowing ratio such as $M = 0.5$ provides the highest adiabatic film cooling effectiveness in the near-hole region, whereas the higher blowing ratio gives better protection in the farther downstream region. However, the trend could be reversed depending mainly on hole arrangement and configuration such as the orientation angle. In the present study, the highest film cooling effectiveness is obtained at the blowing ratio of 0.5 for configuration 3 throughout the measured surface. For configuration 1, however, the blowing ratio of 1.0 yields better protection beyond $x/D \cong 2.0$.

References

Afejuku, W.O., Hay, N., Lampard, D., 1983. Measured coolant distributions downstream of single and double rows of film cooling holes. ASME J. Eng. Power 105, 172–177.

Goldstein, R.J., Eckert, E.R.G., Ramsey, J.W., 1968. Film cooling with injection through holes: adiabatic wall temperature downstream of a circular hole. ASME J. Eng. Power 90, 384–395.

Ekkad, S.V., Zapata, D., Han, J.C., 1997a. Heat transfer coefficients over a flat surface with air and CO_2 injection through compound angle holes using a transient liquid crystal image method. ASME J. Turbomach. 119, 580–586.

Ekkad, S.V., Zapata, D., Han, J.C., 1997b. Film cooling effectiveness over a flat surface with air and CO_2 injection through compound angle holes using a transient liquid crystal image method. ASME J. Turbomach. 119, 587–593.

Honami, S., Shizawa, T., Uchiyama, A., 1994. Behavior of the laterally injected jet in film cooling: measurements of surface temperature and velocity/temperature field within the jet. ASME J. Turbomach. 116, 106–112.

Jabbari, M.Y., Goldstein, R.J., 1978. Adiabatic wall temperature and heat transfer downstream of injection through two rows of holes. ASME J. Eng. Power 100, 303–307.

Kline, S.J., McClintock, F.A., 1953. Describing uncertainties in single sample experiments. Mech. Eng. 75, 3–8.

Lee, S.W., Kim, Y.B., Lee, J.S., 1997. Flow characteristics and aerodynamic losses of film cooling jets with compound angle orientations. ASME J. Turbomach. 119, 310–319.

Ligrani, P.M., Wigle, J.M., Criello, S., Jackson, S.M., 1994. Film cooling from holes with compound angle orientations: part 1—results downstream of two staggered rows of holes with 3d spanwise spacing. ASME J. Heat Transf. 116, 341–352.

Muska, J.F., Fish, R.W., Suo, M., 1976. The additive nature of film cooling from rows of holes. ASME J. Eng. Power, 457–464.

Schmidt, D.L., Sen, B., Bogard, D.G., 1996. Film cooling with compound angle holes: adiabatic effectiveness. ASME J. Turbomach. 118, 807–813.

Sellers Jr., J.P., 1963. Gaseous film cooling with multiple injection stations. AIAA J. 1, 2154–2156.

Sen, B., Schmidt, D.L., Bogard, D.G., 1996. Film cooling with compound angle holes: heat transfer. ASME J. Turbomach. 118, 800–806.

Sinha, A.K., Bogard, D.G., Crawford, M.E., 1991. Gas turbine film cooling: flowfield due to a second row of holes. ASME J. Turbomach. 113, 450–456.